

See discussions, stats, and author profiles for this publication at: <https://www.researchgate.net/publication/7499344>

Antiplasmodial activity of ferrocenyl chalcones: Investigations into the role of ferrocene

ARTICLE *in* EUROPEAN JOURNAL OF PHARMACEUTICAL SCIENCES · MARCH 2006

Impact Factor: 3.35 · DOI: 10.1016/j.ejps.2005.09.007 · Source: PubMed

CITATIONS

71

READS

78

8 AUTHORS, INCLUDING:



Edward Tiekink

Sunway Education Group

2,134 PUBLICATIONS **14,527** CITATIONS

[SEE PROFILE](#)



Mei Lin Go

National University of Singapore

100 PUBLICATIONS **2,157** CITATIONS

[SEE PROFILE](#)

available at www.sciencedirect.comjournal homepage: www.elsevier.com/locate/ejps

Antiplasmodial activity of ferrocenyl chalcones: Investigations into the role of ferrocene

Xiang Wu, Edward R.T. Tiekink, Iouri Kostetski, Nikolai Kocherginsky, Agnes L.C. Tan, Soo Beng Khoo, Prapon Wilairat, Mei-Lin Go*

Department of Pharmacy and Medicinal Chemistry Program of Office of Life Sciences, National University of Singapore, 18 Science Drive 4, Singapore 117543, Singapore

ARTICLE INFO

Article history:

Received 26 April 2005

Received in revised form 2 August 2005

Accepted 22 September 2005

Available online 2 November 2005

Keywords:

Ferrocenyl chalcones

Antiplasmodial activity

Redox properties of ferrocene

QSAR analysis

ABSTRACT

A series of ferrocenyl chalcones were synthesized and evaluated in vitro against *Plasmodium falciparum* (K1) in a [^3H] hypoxanthine uptake assay. Appropriate size, electronic, lipophilic and electrochemical parameters were determined for QSAR analysis. The results showed that the location of ferrocene influenced the ease of oxidation of Fe^{2+} in ferrocene and the polarity of the carbonyl linkage. These parameters were found to influence antiplasmodial activity. A general trend was noted in which compounds with ferrocene adjacent to the carbonyl linkage (series A) were associated with more selective and potent antiplasmodial activities. These compounds had polarized carbonyl linkages, lower lipophilicities and ferrocene rings that were less readily oxidized. The most active analogue was 1-ferrocenyl-3-(4-nitrophenyl)prop-2-en-1-one (**28**) (IC_{50} 4.6 μM , selectivity index 37 against KB3-1 cells). To understand how the redox properties of ferrocene might influence antiplasmodial activity, the oxidant properties of selected compounds were investigated in antioxidant (ABTS $^{++}$) and EPR experiments. The incorporation of ferrocene in the chalcone template was found to enhance its role in processes that involved the quenching and generation of free radicals. Thus, ferrocene may participate in redox cycling and this process may contribute to the antiplasmodial activity of ferrocenyl chalcones. However, the extent to which this property is manifested is also influenced by other physicochemical properties (lipophilicity, polarity, and planarity) of the compound.

© 2005 Elsevier B.V. All rights reserved.

1. Introduction

Ferrochloroquine (Fig. 1), the ferrocene analog of chloroquine, was found to be active against resistant strains of *Plasmodium* (Domarle et al., 1998; Delhaes et al., 2001; Atteke et al., 2003; Chim et al., 2004). Investigations suggested that ferrocene played a role in the accumulation of the drug in the digestive vacuoles or other compartments in the parasite (Domarle et al., 1998). The promising activity of ferrochloroquine prompted investigations into the antiplas-

modial activities of other ferrocene-containing compounds (Biot et al., 2000; Delhaes et al., 2000; Itoh et al., 2000; Wu et al., 2002; Beagley et al., 2003). To date, the contribution of ferrocene to antiplasmodial and other biological properties of ferrocene-containing compounds remain uncertain. Some authors maintained that ferrocene fulfilled a structural role, possibly that of a hydrophobic spacer in place of a phenyl ring (Beagley et al., 2003). Others proposed a more “active” role for ferrocene, namely as a source of ferricenium (Fe^{3+}) or reactive oxygen species that had a direct influence on activity

* Corresponding author. Tel.: +65 68742654; fax: +65 67791554.

E-mail address: phagoml@nus.edu.sg (M.-L. Go).

0928-0987/\$ – see front matter © 2005 Elsevier B.V. All rights reserved.

doi:10.1016/j.ejps.2005.09.007

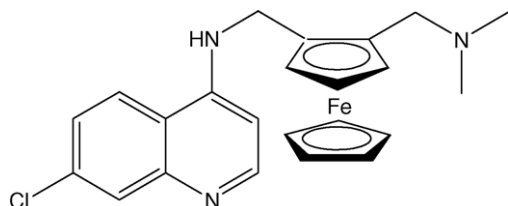


Fig. 1 – Ferrochloroquine.

(Top et al., 2001, 2003; Ong et al., 1992; Osella et al., 2000; Swarts et al., 2001).

The objective of the present study is to systematically assess the contribution of ferrocene to the antiparasmodial activity of ferrocenyl chalcones by a quantitative structure–activity relationship (QSAR) study. Ferrocenyl chalcones are good target compounds because analogs with a range of lipophilicities and electronic properties are readily synthesized. An earlier study had also shown that ferrocenyl chalcones demonstrated a good spread of antiparasmodial activity (Wu et al., 2002). In the present investigation, the correlation between antiparasmodial activity and the physicochemical characteristics of ferrocenyl chalcones was analyzed using multivariate analytical tools (principle component analysis and partial least-squares projection to latent structures). The aim is to obtain a better understanding of the role of ferrocene in the antiparasmodial activity of ferrocenyl chalcones.

2. Experimental

2.1. Materials

The following chemicals were purchased from Sigma-Aldrich (St. Louis, MO): ferrocene aldehyde, acetylferrocene, 5,5-dimethyl-1-pyrroline-N-oxide (DMPO), *N*-tert-butyl- α -phenylnitron (PBN), 2,2,6,6-tetramethylpiperidine-1-oxyl (TEMPO), 6-hydroxy-2,5,7,8-tetramethylchroman-2-carboxylic acid (Trolox), chloroquine diphosphate, 3-(4,5-dimethylthiazol-2-yl)-2,5-diphenyltetrazolium bromide (MTT), diethylenetriamine-pentaacetic acid (DTPA), ethylenediamine-tetracetic acid (EDTA), 2,2'-Azinobis(3-ethylbenzothiazoline-6-sulfonic acid diammonium salt (ABTS) was obtained from Fluka, Steinheim, Germany. Tetrabutylammonium perchlorate (TBAP) was purchased from TCI, Tokyo, Japan.

2.2. Chemistry

The syntheses of ferrocenyl chalcones 1–31 by a base-catalyzed Claisen–Schmidt reaction had been reported (Wu et al., 2002). Compounds 32–44 were synthesized in a similar manner. The reduced ferrocenyl chalcones (R1, R2, R43, R13, R14, R21) were synthesized by catalytic hydrogenation of the corresponding ferrocenyl chalcone (3 mmol) using ethyl acetate as solvent and 10% (w/w) palladium on charcoal (0.1 g) as catalyst. Hydrogenation was carried out in a Parr hydrogenator (30 psi, 4 h, 28 °C) with vigorous agitation. When uptake of hydrogen ceased (usually after 4 h), the catalyst was

removed by filtration and the solvent removed in vacuo. The residue was purified by column chromatography using silica gel (230–400 mesh ASTM) and ethyl acetate–hexane (1:4). All synthesized compounds were characterized by their melting points (uncorrected), ^1H NMR chemical shifts (Bruker DPX 300 MHz spectrometer, reported in δ (ppm), TMS as internal standard), mass spectra (nominal and accurate, VG Micro-mass 7035 E mass spectrometer, electron spray ionization) and elemental analyses for carbon and hydrogen. The purity of selected compounds was further determined by reverse-phase HPLC using two different solvent systems (methanol–water and acetonitrile–water). The yields of the synthesized compounds, melting points and spectroscopic data are given in Tables 1 and 2 (supporting material).

2.3. Evaluation of *in vitro* antiparasmodial activity

The method described by Liu et al. (2001) was followed. Briefly, the inhibition of [^3H] hypoxanthine incorporation by a chloroquine resistant strain of *P. falciparum* (K1) was determined and expressed as its IC_{50} . The test compounds were initially dissolved in DMSO and the final concentration of DMSO in each test well (<0.5%, v/v) did not affect plasmodial growth. Chloroquine was used as a positive control.

2.4. Cytotoxicity measurements

IC_{50} for cytotoxicity was evaluated on a human epidermoid cancer cell line (KB3-1) and Madin–Darby canine kidney (MDCK) cells by the microculture tetrazolium assay described by Alley et al. (1988).

2.5. Determination of lipophilicity by reversed phase HPLC

Lipophilicity was determined experimentally from capacity factors (k') by a reversed phase HPLC method using a LiChrosorb RP-18 (10 μm) column as stationary phase and methanol–water as mobile phase, as described by Liu et al. (2001).

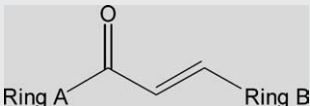
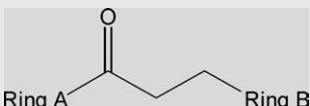
2.6. Determination of the chemical shift of the carbonyl carbon

The chemical shift of the carbonyl carbon in the ferrocenyl and dihydroferrocenyl chalcones was determined by ^{13}C NMR spectroscopy in deuterated chloroform (tetramethylsilane as reference) on a Bruker ACF 300 instrument.

2.7. Cyclic voltammetry

The electrochemical measurements were performed at room temperature (23 °C) on a stripping voltammeter (EG & G Princeton Applied Research, Model 264A) equipped with recorder (Graptec XY, Model WX 2400). The cell was filled with a solution of the test compound (1 mM) in anhydrous acetonitrile containing 0.1 M TBAP and degassed with N_2 , 10 min to eliminate oxygen and water. A glassy carbon electrode served as the working electrode and Ag/AgNO_3 (10 mM in anhydrous acetonitrile containing 0.1 M TBAP)

Table 1 – Antiplasmodial activities and selectivity indices of ferrocenyl chalcones 1–44, and dihydroferrocenyl chalcones

											
No.	Ring A ^a	Ring B	IC ₅₀ (μM) ^b	Selectivity index ^c		No.	Ring A ^a	Ring B	IC ₅₀ (μM) ^b	Selectivity index	
				MDCK ^c	KB3-1 ^d					MDCK ^c	KB3-1 ^d
13	Fc	Ph	19.0	2.9	3.1	1	Ph	Fc	175	0.2	0.4
14		4-MethoxyPh	17.0	1.8	1.2	2	4-MethoxyPh		410	0.2	0.3
15		2,4-DimethoxyPh	18.0	3.9	1.8	3	2,4-DimethoxyPh		24.5	1.5	2.8
16		2-Naphthalenyl	73.5	0.7	0.5	4	2-Naphthalenyl		21.0	2.9	2.5
17		1-Naphthalenyl	72.5	0.5	1.2	5	1-Naphthalenyl		47.4	2.6	2.7
19		4-HydroxyPh	20.6	5.0	1.4	7	4-HydroxyPh		36.0	1.7	1.9
21		4-ChloroPh	14.5	3.6	2.1	43	4-ChloroPh		78.5	–	–
25		4-FluoroPh	12.1	5.3	18	44	4-FluoroPh		32.7	–	–
38		2-Pyridinyl	58.3	–	0.6	32	2-Pyridinyl		53.6	–	12
18		3-Pyridinyl	17.0	2.9	1.2	6	3-Pyridinyl		4.6	5.3	8.6
39		4-Pyridinyl	14.0	–	4.1	33	4-Pyridinyl		31.6	–	4.0
40		2-NitroPh	53.8	–	2.5	34	2-NitroPh		39.4	–	3.4
41		3-NitroPh	41.7	–	1.0	35	3-NitroPh		36.5	–	0.6
28		4-NitroPh	5.1	14	37	36	4-NitroPh		61.7	–	–
42		2,4-Dimethyl-aminoPh	58.7	–	2.9	37	2,4-DimethylaminoPh		131	–	0.6
20		4-MethylPh	14.7	0.5	0.6	8	2,4-DihydroxyPh		31.5	2.9	3.2
22		3-ChloroPh	36.2	1.5	1.3	9	2-HydroxyPh		73.5	0.7	1.5
23		2-ChloroPh	42.4	1.6	1.5	10	2,3,4-TrimethoxyPh		22.5	2.3	3.4
24		2,4-DichloroPh	29.4	2.3	1.7	11	4-EthoxyPh		200	0.2	0.5
26		2,4-DifluoroPh	23.2	2.9	6.7	12	4-ButoxyPh		80	1.3	1.2
27		4-Trifluoro-methylPh	58.4	0.5	1.2	45	Fc		26.9	–	–
29		4-CyanoPh	26.5	3.3	11	C1	Ph	Ph	47.4	–	–
30		3-Quinoliny	18.2	3.7	0.9	C6	3-Pyridinyl		24.9	–	–
31		4-Quinoliny	14.0	14	7.5	C28	Ph	4-NitroPh	18.5	–	–
											
No.	Ring A	Ring B	IC ₅₀ (μM) ^b	Selectivity index		No.	Ring A	Ring B	IC ₅₀ (μM) ^b	Selectivity index	
				MDCK ^c	KB3-1 ^d					MDCK ^c	KB3-1 ^d
R13	Fc	Ph	132	–	0.9	R1	Ph	Fc	27.2	–	–
R14		4-methoxyPh	199	–	0.8	R2	4-methoxyPh		67.2	–	–
R21		4-chloroPh	191	–	2.0	R43	4-chloroPh		35.6	–	–

^a Series A compounds have ferrocene (Fc) as ring A. Series B compounds have ferrocene (Fc) as ring B. Ph: phenyl.
^b IC₅₀ values for inhibition of [³H] hypoxanthine uptake into *P. falciparum* (K1). IC₅₀ for chloroquine = 0.26 μM. IC₅₀ for ferrocene = 71 μM. All readings are the average of two or more separate determinations.
^c Selectivity index = IC₅₀ for cytotoxicity against MDCK cells/IC₅₀ *P. falciparum*.
^d Selectivity index = IC₅₀ for cytotoxicity against KB3-1 cells/IC₅₀ *P. falciparum*.

was used as reference electrode. The working electrode was polished before measurements were made at a scan rate of 50 mV s^{−1}. Cathodic peak potentials were measured relative to the Ag/AgNO₃ reference electrode.

2.8. X-ray crystallography

Crystallographic data of compounds **1**, **12**, and **28** were collected on a Bruker AXS SMART CCD diffractometer using Mo Kα radiation at 223 K so that θ_{\max} was 30.1° (30.0° for **12**). Data were reduced (SMART & SAINT, Ver. 5.6, Bruker AXS Inc., Madison, WI) and corrected for absorption effects

(SADABS) (Blessing, 1995). The structures were solved by heavy-atom methods (PATTY in DIRDIF) (Beurskens et al., 1992) and refined (anisotropic displacement parameters, H atoms in calculated positions, and a weighting scheme of the form $w = 1/[\sigma^2(F_o^2) + aP^2 + bP]$, where $P = (F_o^2 + 2F_c^2)/3$) on F² (SHELXL-97) (Sheldrick, 1997). Structures are drawn with ORTEP at 50% displacement ellipsoids. Data manipulation was with teXsan (Structure Analysis Package, Molecular Structure Corporation, Houston, TX) and data have been deposited at the CCDC with deposition numbers 257045 (**1**), 257044 (**12**) and 257043 (**28**). Crystal data of **1**, **12** and **28** are presented in Table 3 (supporting material).

Table 2 – Selected bond distances (Å), bond angles (°) and torsion angles (°) of compounds 1, 12, and 28

Parameter	1	12	28
C1–O1	1.216 (4)	1.227 (3)	1.219 (3)
C1–C2	1.485 (4)	1.476 (3)	1.480 (3)
C2–C3	1.324 (4)	1.325 (3)	1.318 (3)
C1–C11	1.496 (4)	1.491 (3)	1.464 (3)
C3–C31	1.456 (4)	1.448 (3)	1.462 (3)
Fe–Cg1 ^a	1.645 (2)	1.640 (1)	1.648 (1)
Fe–Cg2 ^a	1.652 (2)	1.649 (1)	1.654 (1)
O1–C1–C2	120.9 (3)	121.3 (2)	121.6 (2)
O1–C1–C11	119.9 (3)	120.0 (2)	121.3 (2)
C2–C1–C11	119.2 (3)	118.8 (2)	117.1 (2)
C1–C2–C3	119.8 (3)	121.3 (2)	121.3 (2)
C2–C3–C31	126.2 (3)	126.1 (2)	127.6 (2)
C11–C1–C2–C3	–176.9 (3)	175.4 (2)	177.6 (2)
C12–C11–C1–C2	170.6 (3)	–163.0 (2)	–3.4 (3)
C1–C2–C3–C31	179.6 (3)	–178.1 (2)	–174.8 (2)
C2–C3–C31–C32	15.7 (5)	–12.2 (4)	–175.0 (2)
Cg1...Fe...Cg2 ^a	179.5 (1)	179.5 (1)	178.7 (1)

^a Cg1 and Cg2 are the ring centroids of the cyclopentadienyl rings C31–C35 and C36–C40, respectively.

2.9. Molecular modeling methods

The series A and B ferrocenyl chalcones were constructed in silico using the crystallographic parameters of **28** and **1**, respectively. For each compound, the bond between ferrocene and the adjacent carbon was constrained and the charge on the iron was assigned +2 by the Gasteiger–Huckel method. Other charges (carbonyl carbon and oxygen) were similarly assigned. Minimization was performed using the standard Sybyl 6.6 molecular mechanics force field MMFF94 (Tripos Associates, St. Louis, MO), with a 0.001 kcal mol^{–1} energy gradient convergence criterion. Using this approach, the minimized structure of **12** had similar dimensions as its crystal structure, thus validating the method employed for the molecular modeling of the test compounds.

2.10. Scavenging of ABTS^{•+}

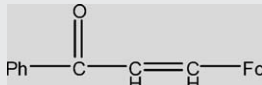
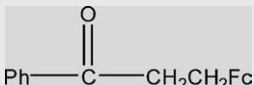
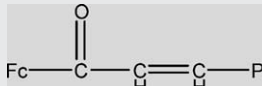
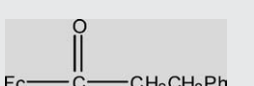
The method of Re et al. (1999) was followed. Briefly, stock solutions of ABTS (7 mM) and potassium persulfate (0.245 M) were prepared in distilled water. Aliquots of ABTS (1 ml) and potassium persulfate (10 µl) were mixed to give a stock solution that was kept in the dark at 23 °C for 16 h to optimize the production

of the radical cation (ABTS^{•+}). The solution was then diluted with PBS (pH 7.4) to an absorbance of 0.70 (±0.02) at 734 nm. An aliquot of the test sample (10 µl, freshly prepared in 80% ethanol) was mixed with the ABTS^{•+} solution (990 µl) in a 1 ml cuvette and absorbance was recorded over a period of 5 min. At least three concentrations of test compound and a known antioxidant (Trolox) were determined over the concentration range of 2.5–15 µM. Scavenging ability was determined from the reduction in the absorbance of ABTS^{•+} after 5 min at a specific concentration of test compound. At least two repeats were made for each concentration. The plot of %scavenging activity versus concentration of test compound gave a straight line whose gradient was determined. Trolox equivalent antioxidant capacity (TEAC) of the test compound was obtained by dividing the gradient of its line by the gradient of the line obtained with Trolox under similar conditions. TEAC indicates how many times more active the compound was as a radical scavenger compared to Trolox.

2.11. Spin trapping measurements

Spin trapping experiments were carried out to identify the radicals produced when the ferrocenyl chalcones were dissolved in aqueous media. DMPO was treated before use with activated charcoal to remove paramagnetic impurities. PBN was used as received. Stock solutions (1 mM) of the spin traps were prepared in deionized water and kept refrigerated and protected from light. The test compounds were prepared in DMSO and diluted to the desired concentration with deionized water. The concentration of DMSO in the final solutions was 1% (v/v). Chelating agents DTPA (for DMPO) and EDTA (for PBN) were added (10^{–3} M) to the final solutions. The test compound and spin trap were incubated for 45 min (22 °C) in an open flask containing 1.5 ml of reaction mixture in which the final concentration of spin trap and test compound were 100 mM and 100 µM, respectively. About 600 µl of the reaction mixture was transferred at 5 min intervals to a standard quartz flat cell for measurement, after which the solution was returned to the incubation mixture. Spectra were recorded on a Bruker spectrometer (Bruker BioSpin GmbH, Rheinstetten/Karlsruhe, Germany, Elexsys Series E500 CW-EPR X-band, 9–10 GHz) with SuperX TE₁₀₂ mode cavity. Instrument settings were: modulation frequency, 100 KHz; modulation amplitude, 1 G; receiver gain, 60 dB; time constant, 81.9 ms; sweep rate, 149.4 G/min; microwave frequency, ≈9.75 GHz; microwave power, 20 mW. Manganese in magnesium oxide

Table 3 – ¹³C NMR chemical shifts of carbonyl carbon in ferrocenyl chalcones, and their reduced analogs

Compound	Chemical shift δ (ppm) ^a	Compound	Chemical shift δ (ppm) ^a
	189.86		199.51
	192.95		203.10

^a Determined in deuterated chloroform as solvent and TMS as internal standard on 300 MHz Bruker ACF 300 spectrometer.

marker and spin standard TEMPO at final concentrations of 5, 10, 50 and 100 μM , were used to quantify the nitroxide spin adducts.

2.12. Statistical methods

Multivariate data analyses were carried out using SIMCA-P version 8.0 (Umetrics AB, Umea, Sweden) with default settings. Statistical analyses were carried out on SPSS 11 (SPSS Inc., Chicago, IL).

3. Results

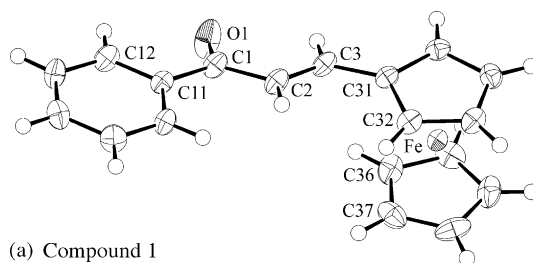
3.1. Syntheses of ferrocenyl chalcones

Table 1 lists the structures of the ferrocenyl chalcones investigated in this study. They were synthesized by a base-catalyzed Claisen–Schmidt condensation using commercially available aldehydes and ketones (Scheme 1). The synthesis of compounds 1–31 had been described earlier (Wu et al., 2002) and the remaining compounds 32–44 were synthesized in a similar manner. Reduction of the α,β -unsaturated double bond was achieved by catalytic hydrogenation to give dihydro ferrocenyl chalcones R1, R2, R13, R14, R21, R43. Details on the yields, melting points, spectroscopic and other characteristics of the synthesized compounds are given in Tables 1 and 2, supporting materials.

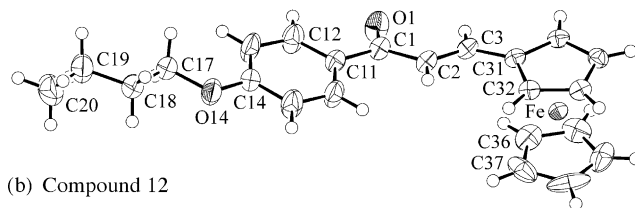
3.2. X-ray crystal structures of compounds 1, 12 and 28

The crystal structures of three ferrocenyl chalcones (1, 12 and 28) were established unambiguously in the solid state by X-ray crystallography. Selected geometric parameters and ORTEP structures of compounds 1, 12 and 28 are given in Table 2 and Fig. 2, respectively. An examination of the derived torsion angles (C11–C1–C2–C3 and C1–C2–C3–C31) confirmed the overall planarity of the central $\alpha\beta$ -unsaturated carbonyl linker, in keeping with earlier reports (Rastelli et al., 2000; Lopez et al., 2001). The data suggested limited delocalization of π -electron density over the central chromophore despite the presence of planarity. This was seen from the length of the carbonyl bond (C1–O1) which was as expected for formal carbonyl bonds, and the double bond (C2–C3) which was typical of carbon–carbon double bonds. Angles subtended at the C1 (O1–C1–C2, O1–C1–C11) and C2 (C1–C2–C3) atoms deviated only marginally from the ideal angle of 120° . By contrast, significant deviations were apparent about the C3 atom (C2–C3–C31), an effect that was attributed to the presence of the C31 atom of the phenyl (28) or ferrocene ring (1, 12).

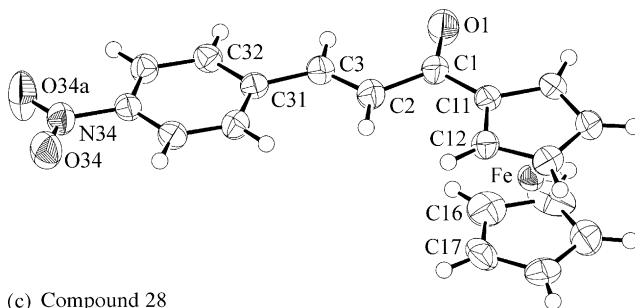
The torsion angle C12–C11–C1–C2 measured the orientation of ring A with respect to the $\alpha\beta$ -unsaturated carbonyl



(a) Compound 1



(b) Compound 12

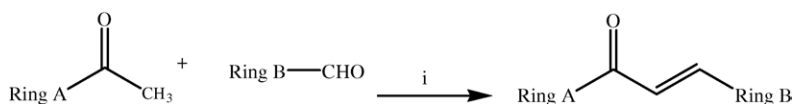


(c) Compound 28

Fig. 2 – Molecular structures and crystallographic numbering schemes for: (a) 1, (b) 12, and (c) 28.

linker. When ring A was phenyl (as in 1 and 12), there was marked deviation from the central linker (by 10 – 17°) as compared to when ring A was ferrocene (28, 3° deviation). By contrast, when the orientation of ring B was examined (C2–C3–C31–C32), the association of planarity with ferrocene was no longer observed. In fact, the ferrocene ring B in 1 and 12 were twisted to a greater extent (12 – 15°) than the phenyl ring B of 28 (5°). It would seem that the presence of ferrocene as ring A influenced the overall planarity of the molecule. Thus, of the three compounds, 28 (a series A compound) was the most planar with respect to the orientation of both rings A and B and the central chromophore.

The cyclopentadienyl rings of ferrocene were symmetrically disposed about the iron atom. Viewed down the $\text{Cg1} \cdots \text{Fe} \cdots \text{Cg2}$ axis, where Cg1 and Cg2 are the ring centroids of the substituted and unsubstituted cyclopentadienyl rings, respectively, the two rings were almost eclipsed in the three compounds.



Scheme 1 – Synthesis of ferrocenyl chalcones (series A and series B): (i) KOH, ethanol, RT. Ring A: ferrocene; ring B: substituted phenyl, naphthalene, pyridine, quinoline in Series A. This is reversed in Series B (Table 1).

The dimensions of **28** were used to construct ferrocenyl chalcones that have ferrocene as ring A (series A) in silico, while **1** was used in a similar capacity for compounds with ferrocene as ring B (series B).

3.3. Physicochemical characterization of ferrocenyl chalcones

The ferrocenyl chalcones (**1–44**) were characterized by their lipophilicities, size and electronic properties. Lipophilicity was assessed from experimentally determined HPLC-derived capacity factors ($\log k_w$, pH 7.0). The ferrocenyl chalcones were lipophilic molecules with $\log k_w$ ranging from 2.7 to 5.1. Comparison of selected series A and B compounds of comparable sizes (evaluated from area and volume parameters) indicated that series A compounds ($\log k_w = 3.63 \pm 0.56$, $n = 15$) were less lipophilic than series B compounds ($\log k_w = 3.87 \pm 0.46$, $n = 15$). The difference was significant at $p = 0.003$ (paired t-test, two-tailed).

The electronic properties of the ferrocenyl chalcones were characterized in several ways. The charges on the oxygen and carbon atoms of the carbonyl bond were determined by the Gasteiger–Hückel method from energy minimized structures and reported as the difference in charge between the two atoms. A large charge difference indicated that the carbonyl bond was polarized to a greater extent. It was noted that the carbonyl linkage in series A was polarized to a greater degree than the compounds in series B (paired t-test, $p < 0.001$).

The ^{13}C chemical shift of the carbonyl carbon was also determined. The chemical shift reflected the degree of polarization of the carbonyl bond and would be influenced in part by neighbouring electron donating and withdrawing groups. For example, the replacement of the methyl group of acetone or acetaldehyde by a phenyl group caused an upfield shift of the carbonyl carbon signal, as did α,β -unsaturation (Silverstein and Webster, 1997), indicating that charge delocalization from phenyl and the double bond rendered the carbonyl carbon less electron deficient. In the same way, electron donating groups on rings A or B would be expected to reduce the electron deficient character of the carbonyl carbon (upfield shift) while electron withdrawing groups would have an opposite effect (downfield shift). Besides electronic factors, the chemical shift of the carbonyl carbon was also affected by the orientation of the ring A with respect to the carbonyl bond. In particular, if ring A is constrained out-of-plane, a shielding effect

may be induced on the carbonyl bond and an upfield shift will be observed. The chemical shift of the carbonyl carbon (192.64 ± 0.42 , $n = 20$) in series A was found to be statistically different from the series B analogues (189.34 ± 2.23 , $n = 20$) by the paired t-test ($p < 0.001$).

Ferrocene and the carbonyl linkage in ferrocenyl chalcones are susceptible to oxidation–reduction reactions. Ferrocene is oxidized to ferricenium via a reversible one-electron reaction while the carbonyl group undergoes irreversible electrochemical reduction (Hoccek et al., 2004; Aston and Fry, 2004). The ease with which these processes occur had been linked to biological activity. Chibale et al. (2000) noted that the antiparasmodial activities of some amine and urea analogs of ferrochloroquine were correlated to the oxidation potential of ferrocene. The reducibility of the carbonyl function was found to influence the cytotoxicity of Mannich-base chalcones and conformationally restricted chalcones (Dimmock et al., 1998, 2001). In view of these findings, the oxidation ($E_p^{\text{Fc.oxi.}}$) and reduction ($E_p^{\text{Fc.red.}}$) potentials of ferrocene and the reduction potential ($E_p^{\text{C=O.red.}}$) of the carbonyl bond were determined by cyclic voltametry. The formal potential E'_o (mean of $E_p^{\text{Fc.oxi.}}$ and $E_p^{\text{Fc.red.}}$) and ΔE_p ($= E_p^{\text{Fc.oxi.}} - E_p^{\text{Fc.red.}}$) were also derived. ΔE_p measured the reversibility of the one-electron transfer reaction in ferrocene and has a theoretical value of 0.060 V. Experimentally, a mean value of 0.062 V (± 0.07 , $n = 44$) was obtained, indicating that the reaction was reversible in the ferrocenyl chalcones. The formal potentials of the series B compounds were significantly lower than their series A analogues (paired t-test, $p < 0.001$) but the reduction potentials of the carbonyl bond in series A and B were not statistically different.

The physicochemical parameters ($\log k_w$, Connolly volume and surface area, charge difference of the carbonyl carbon and oxygen atoms, ^{13}C chemical shift of carbonyl carbon, $E_p^{\text{Fc.oxi.}}$, $E_p^{\text{Fc.red.}}$ of ferrocene, $E_p^{\text{C=O.red.}}$, E'_o and ΔE_p) are presented in Table 4, supporting material. The parameters were used for QSAR analysis, except for ΔE_p which was excluded because its value remained fairly constant for the entire series of compounds.

3.4. In vitro antiplasmodial activity against Plasmodium falciparum K1

Table 1 lists the concentration (IC_{50}) of test compound required to inhibit by 50% the uptake of $[^3\text{H}]$ hypoxanthine by chloroquine-resistant *P. falciparum* K1. The most active com-

Table 4 – Summary of PLS models used for QSAR analysis of ferrocenyl chalcones

	Model 35 (without 6)	Model 10 (with 6)
Compounds	All except naphthalenes (4, 5, 16, 17), Ring A pyridines (6, 32, 33), outliers (2, 7, 20); $N = 34$	All except naphthalenes (4, 5, 16, 17), Ring A pyridines (32, 33), outliers (2, 7, 20); $N = 35$
X variables	$\log k_w$, E'_o , ^{13}C chemical shift, $E_p^{\text{Fc.red.}}$, charge difference ($\text{C}=\text{O}$)	$\log k_w$, E'_o , ^{13}C chemical shift, $E_p^{\text{Fc.red.}}$, surface area
Model statistics	$r^2 = 0.43$; $q^2 = 0.39$	$r^2 = 0.33$; $q^2 = 0.28$
Test set	Compounds 14, 23, 34, 37, 39 and 43. X variables as above. Significant two component model, $q^2 = 0.81$.	Compounds 19, 24, 34, 36, 40 and 43. X variables as above. Significant two component model, $q^2 = 0.71$.
RMSEP ^a	0.30	0.34

^a Root-mean square error of prediction. This is the level of predictability obtained when the test set was used to predict the activity of the remaining (unselected) compounds in the model.

pounds were 1-(3-pyridinyl)-3-ferrocenylprop-2-en-1-one (**6**) and 1-ferrocenyl-3-(4-nitrophenyl)prop-2-en-1-one (**28**) which had IC_{50} values of 4.6 and 5.1 μM , respectively. 2-Pyridinyl (**32**) and 4-pyridinyl (**33**) analogs of **6** were less active, as were the 2- and 3-nitro analogs of **28**. Clearly, positional isomerism of the nitro and pyridine rings affected activity. The cytotoxicities of compounds **6** and **28** were determined against two mammalian cell lines—human epidermoid carcinoma (KB) cells and Mardin–Darby canine kidney (MDCK) cells and expressed as selectivity indices (IC_{50} mammalian cell line/ IC_{50} plasmodium) in Table 1. Most of the ferrocenyl chalcones were selectively active against *Plasmodium* (Table 1). Of the two active compounds, **28** had the higher selectivity index when tested on KB (SI = 37) and MDCK (SI = 14) cells. Compound **6** was less selective against *Plasmodium*.

Among the ferrocenyl chalcones, there are 15 pairs of compounds in which the rings A and B are “switched”. Each pair had similar size parameters but differed in their $\log k_w$ values, with the series A compound associated with a lower lipophilicity than its series B analog. In addition, statistically significant differences in redox properties of the ferrocene and the polarizability of the carbonyl bond were noted. When antiparasmodial activities of these compounds were compared, the member with ferrocene as ring A (series A) was generally more active than the corresponding member with ferrocene as ring B (series B) in 9 out of the 15 isomeric pairs. The nature of the substituent on the phenyl ring did not markedly influence this trend and compound pairs with electron withdrawing (4-chloro **43** and **21**; 4-nitro **36** and **28**) and electron donating substituents (4-methoxy **2** and **14**; 4-hydroxy **7** and **19**; 4-dimethylamino **37** and **42**) consistently showed greater activity in the series A compound. However, exceptions were found among compounds with pyridine and naphthalene rings. In these cases (**4** and **16**; **5** and **17**; **6** and **18**), greater activity was observed in the series B compound.

Reduction of the α,β -unsaturated bond in ferrocenyl chalcone had varied effects on antiparasmodial activity. A significant decrease in activity was observed on reduction of the series A compounds (**R13**, **R14** and **R21**) but a marked improvement was evident for the reduced series B compounds (**R1** and **R43**). Other reports had also noted the ambiguous effects on antiparasmodial activity on saturating the α,β -unsaturated linkage in chalcones (Li et al., 1995; Nielsen et al., 1998).

3.5. QSAR analysis: PCA and PLS

Of the 15 pairs of isomeric ferrocenyl compounds investigated, nine pairs had greater antiparasmodial activity associated with the series A compound. This trend suggested that the location of ferrocene in the chalcone framework may be a contributing factor to antiparasmodial activity. A casual examination of the physicochemical parameters showed differences in lipophilicities, formal potential (E'_0), chemical shift of the carbonyl carbon and charge distribution of the carbonyl bond of the series A and B compounds. Ferrocene in series A compounds were generally more resistant to electron loss from Fe^{2+} (larger E'_0 values). In addition, the carbonyl bonds in series A were more polarized as seen from the larger charge difference between carbonyl carbon and oxygen atoms and the downfield ^{13}C chemical shifts. In order to arrive at a more

quantitative assessment of these differences, principal component analysis (PCA) was applied. PCA is a pattern recognition technique that aims at summarizing information residing in the original data into a form that can reveal relationships between the compounds and the parameters used in their characterization (Livingstone, 1995). It is particularly useful in situations where some of the independent variables may be correlated, as in this investigation. PCA would confirm if series A and B compounds do indeed differ significantly in their physicochemical properties, and if so, which properties contributed to the observed differences.

When PCA was applied to the nine physicochemical parameters (Table 4, supporting materials, excluding ΔE_p) of the ferrocenyl chalcones ($n = 44$), a significant two-component model ($r^2 = 0.75$, $q^2 = 0.55$) was obtained. This meant that the properties captured by these components could account for 75% of the observed variation among the compounds, with a predictability level of 55%. The loading plot of the model identified the redox properties ($E_p^{Fc_{oxi}}$, $E_p^{Fc_{red}}$, E'_0) of ferrocene, difference in charges of oxygen and carbon in the carbonyl bond and chemical shift of carbonyl carbon (in order of decreasing importance) as significant contributors to the first component. The second component represented size parameters and lipophilicity (Fig. 3a). The reduction potential of the carbonyl bond ($E_p^{C=O_{red}}$) did not contribute to either component.

The score plot shows the distribution of the compounds according to their principal components (Fig. 3b). Clustering of series A compounds was observed on one side of the plot (except for the nitro compounds **40** and **42**) while the series B compounds were spread out on the opposite side. Clearly, some physicochemical properties of the ferrocenyl chalcones were affected by the location of ferrocene as ring A or ring B. PCA identified these properties to be those that contributed significantly to the principal components, namely the redox properties of ferrocene and the charge distribution on the carbonyl bond. In view of this finding, it was of interest to understand why these properties were different in series A and B compounds.

The carbonyl bond was more polarized in series A than in series B as shown from the charge difference between the carbon and oxygen atoms of the carbonyl bond (series A 0.228 ± 0.027 ; series B 0.155 ± 0.016 , $p < 0.001$) and the deshielded carbonyl carbon in series A (series A: δ 192.64 \pm 0.42 ppm; series B: δ 189.34 \pm 2.23; $p < 0.001$).

The deshielding of the carbonyl carbon in series A compounds may be explained by steric and electronic factors. The X-ray crystal data of **28**, a representative series A compound, showed that the ferrocene ring and the carbonyl bond in the central linker were closely aligned on the same plane (Section 3.2). When orientated in this manner, the carbonyl carbon would fall within the region of the paramagnetic field current and be deshielded. The geometrical parameters of **1** and **12** which belonged to series B had a greater deviation from planarity and these compounds had more shielded carbonyl carbons. Thus the orientation of ferrocene and the carbonyl function could have influence the extent of deshielding experienced by the carbonyl carbon.

To have a better understanding of the electronic effects of ferrocene, the chemical shifts of the carbonyl carbon in selected ferrocenyl chalcones and their reduced analogues

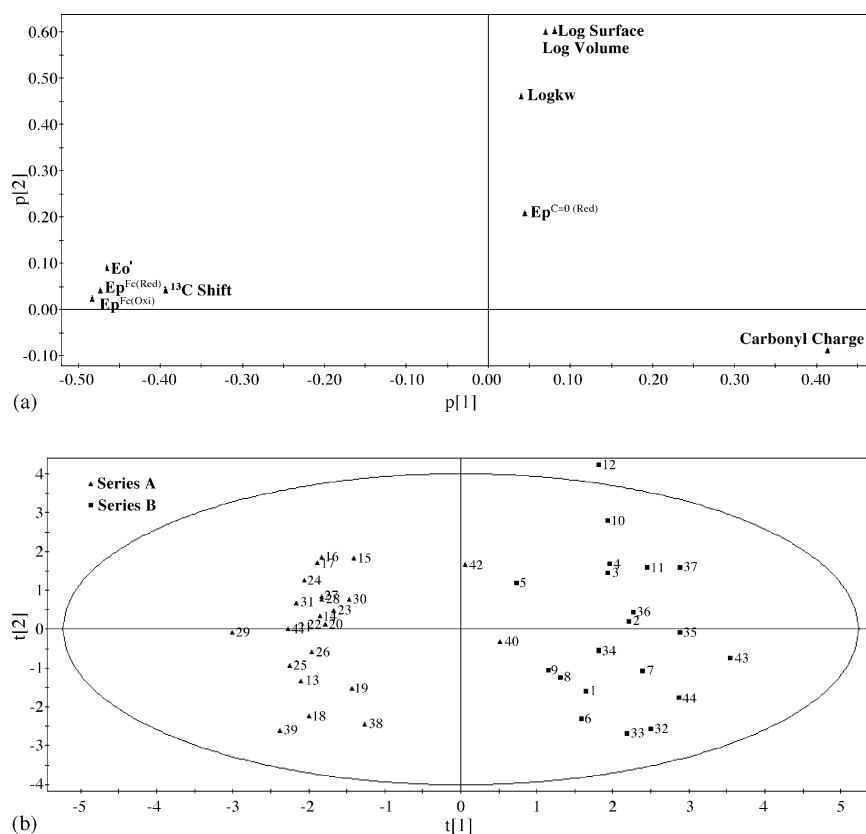


Fig. 3 – (a) Loading plot of first and second principal components (p_2 vs. p_1) of ferrocenyl chalcones ($n = 44$, nine parameters). The loadings reveal the magnitude (large or small correlation) and the manner (positive or negative) in which the measured variables contribute to the formation of the scores. The main variables contributing to the first and second components are the redox parameters of ferrocene and size parameters (volume, surface area, lipophilicity), respectively. (b) Score plot of principal components t_1 vs. t_2 for ferrocenyl chalcones ($n = 44$, nine parameters). Compounds to the left of the midline are series A ferrocenyl chalcones ($n = 20$) and those to the right of the midline are series B ferrocenyl chalcones ($n = 24$). The eclipse corresponds to the confidence region based on Hotelling T^2 (0.05). Compound 12 is an outlier as it lies outside the eclipse but its omission did not significantly improve predictability.

were compared (Table 3). Reduction of the α,β -unsaturated linkage resulted in deshielding of the carbonyl carbon. The data suggested that electron donation from the α,β -unsaturated linkage played a role in determining electron density on the carbonyl carbon. A carbonyl carbon was more deshielded when adjacent to ferrocene, as seen from the chemical shifts of R1 (199.51), R13 (203.10) and 1 (189.86), 13 (192.94). Notwithstanding steric factors, this may reflect differences in the electron donating abilities of the two rings, with ferrocene taking on a less electron-donating role when adjacent to carbonyl. This may also imply resistance to electron loss from Fe^{2+} (larger E'_0) when ferrocene was ring A. Indeed, the ferrocene ring in series A was found to have a higher formal potential ($0.353 \text{ V} \pm 0.035$) as compared to series B ($0.222 \text{ V} \pm 0.023$) compounds.

One possible explanation may be that when ferrocene was adjacent to the carbonyl function in series A, the electron withdrawing effect of the carbonyl group lowered the electron density at Fe^{2+} , thus making electron loss from the metal ion less likely, leading to a higher E'_0 . Hocek et al. (2004) explained the resistance to electron loss in ferrocene linked to an electron withdrawing ethynyl group in this manner. But if this

was the case for the ferrocenyl chalcones, then the carbonyl linkage should not be so markedly polarized in series A compounds. More investigations would be required to explain the greater resistance of the ferrocene ring A to oxidation.

The next question that required consideration was how differences in physicochemical properties influenced antiparasitodal activity. Partial least squares projection to latent structures (PLS), a regression extension of PCA, was used to answer this question (Livingstone, 1995). The segregation of series A and series B compounds in the PCA score plot implied that the two series should be handled separately when analyzed for SAR. However, neither series A nor series B yielded meaningful PLS models when analyzed separately. On the other hand, when compounds with naphthalene (4, 5, 16 and 17), pyridine (6, 18, 32, 33, 38 and 39) and quinoline rings (30 and 31) were omitted from the combined series, a significant one-component model was obtained. But this was a weak model that could account for only 31% of the observed variation and at a low level of predictability ($q^2 = 0.25$). Further investigations showed that the quinolines 30, 31 and pyridines 18, 38, 39 (pyridine is ring B in these compounds) could be included with little change to the model statistics ($r^2 = 0.34$;

$q^2 = 0.26$). However, this model excluded compound 6, one of the two most active compounds. Thus, it was appropriate to explore the effect of including this compound in the final model. These investigations are summarized in Table 4. The basic steps involved in “refining” the model were omission of outliers (compounds with large differences in predicted and observed values) and removal of variables that did not significantly contribute to the model. The validity of the final model was assessed by selecting a test set and using it to predict the activity of the remaining compounds. The test set was selected from the original compounds used to develop the final models and their characteristics are listed in Table 4.

Table 4 shows that a more robust model ($q^2 = 0.39$) resulted when compound 6 was excluded. This model (35) predicted good activity for compounds that were less lipophilic, have polarized carbonyl bonds and ferrocene rings that were resistant to oxidation. The level of prediction, as assessed from the root-mean-square error of prediction (RMSEP) was moderately good (RMSEP = 0.30). Inclusion of compound 6 reduced the predictability of the model (10, $q^2 = 0.28$, RMSEP = 0.34) and did not change the profile required for good activity. This could be seen from the coefficient plots of the two models which showed the influence of selected parameters on antiplasmodial activity (Fig. 4). Despite the lower q^2 associated with model 10, the test set derived from it was able to predict the activity of the remaining compounds with a slightly higher level of confidence (RMSEP = 0.34).

3.6. Role of ferrocene in antiplasmodial activity

QSAR has revealed a general trend in which better activity was associated with the series A compounds, which also had ferrocene rings that were more resistant to oxidation. These findings suggested a role for ferrocene that goes beyond that of a spacer group or a replacement ring for phenyl. Thus, it was of interest to investigate the likely role of ferrocene in antiplasmodial activity. Since the oxidizability of ferrocene was emphasized in QSAR, the oxidant properties of selected ferrocenyl chalcones were investigated.

Electron transfer from ferrocenyl chalcones was investigated using the long-lived radical cation 2,2'-azino-bis(3-ethylbenzothiazoline-6-sulfonic acid) [$\text{ABTS}^{\bullet+}$]. Compounds that donated electrons to $\text{ABTS}^{\bullet+}$ would quench its absorbance and the extent to which absorbance was diminished reflected the scavenging or electron donating ability of the target compound. The scavenging ability of the compound was reported in terms of its TEAC which measured its effectiveness as a radical scavenger compared to a standard antioxidant Trolox (Table 5).

There was evidence to support an important role for ferrocene in the radical scavenging activity of the ferrocenyl chalcones as seen from the negligible scavenging activities of the phenyl analogues (C6, C28) as compared to their ferrocenyl counterparts 6 and 28, respectively. In addition, 1,3-diferrocenyl chalcone showed impressive scavenging activity (TEAC 5.2) as compared to its phenyl analogue (1,3-diphenylprop-2-en-1-one has no observable TEAC value). Among the ferrocenyl chalcones, 8 had the highest TEAC (2.39). Interestingly, its phenyl analog (C8) also has an exceptionally good TEAC value (1.16). Moreover, the number and

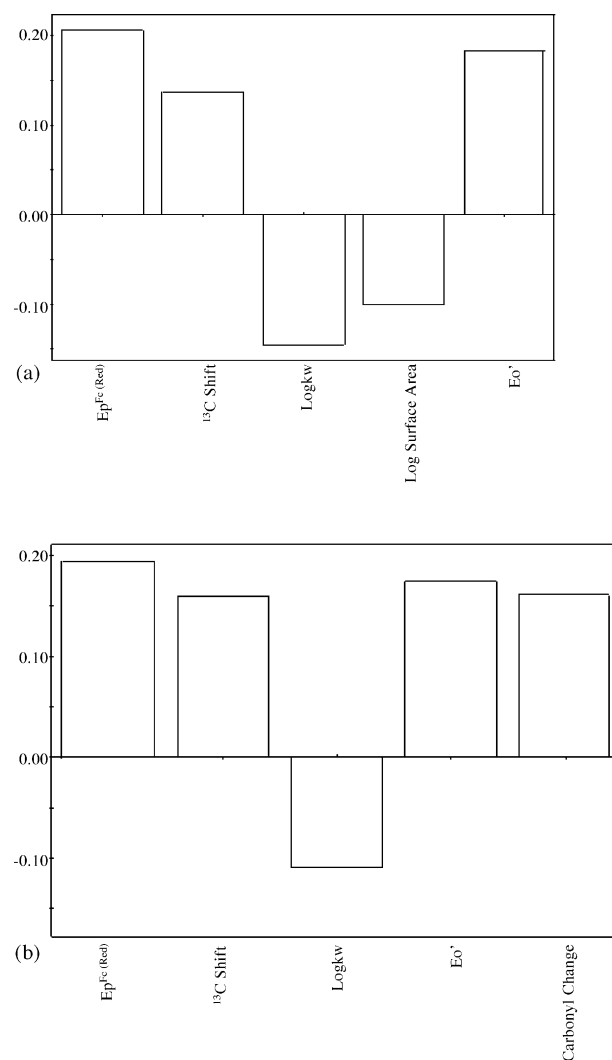
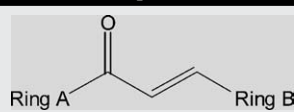


Fig. 4 – (a) Coefficients plot for PLS model (10) derived from 35 ferrocenyl chalcones and five variables ($r^2 = 0.33$; $q^2 = 0.28$). Compound 6 is included in this model. Parameters with positive coefficients are directly related to activity. Parameters with negative coefficients are inversely related to activity. (b) Coefficients plot for PLS model (35) derived from 34 ferrocenyl chalcones and five variables ($r^2 = 0.43$; $q^2 = 0.39$). Compound 6 is excluded from this model.

position of hydroxyl groups on the phenyl ring A of C8 played a pivotal role, as seen from the lower TEAC values of 2'-hydroxychalcone (0.66) and 4'-hydroxychalcone (0.26). Thus, the good scavenging activity of 8 may be attributed to the combined presence of appropriately placed phenolic hydroxyl groups and ferrocene in the molecule.

The ability of Fe^{2+} in ferrocene to donate electrons to $\text{ABTS}^{\bullet+}$ implied that electrons could be donated to other suitable acceptors with the formation of free radicals. The reactions of Fe^{2+} with oxygen (Haber–Weiss reaction) and hydrogen peroxide (Fenton reaction) are known to generate reactive oxygen species (superoxide, hydroxyl radical) that can inflict considerable biological damage. Thus, free radical for-

Table 5 – Scavenging of ABTS radical cation and formation of free radicals determined by EPR by ferrocenyl chalcones and related compounds


	Ring A	Ring B	TEAC ^a	PBN adducts (μM) ^b	Rate of PBN adduct formation ^c (10 ⁻⁸ M min ⁻¹)
13	Fc	Ph	0.65	2.00	11.4
14		4-CH ₃ OPh	1.16		
15		2,4-(CH ₃ O) ₂ Ph	1.26		
16		2-Naphthalenyl	0.35		
18		3-Pyridinyl	1.27		
19		4-OHPh	0.83		
27		4-CF ₃ Ph	0.68	0.79	1.5
28		4-NO ₂ Ph	0.58	0.55	1.6
29		4-CNPh	0.35		
39		4-Pyridinyl	1.48		
1	Ph	Fc	0.98	1.21	2.7
2	4-CH ₃ OPh		0.49		
3	2,4(CH ₃ O) ₂ Ph		0.78		
4	2-Naphthalenyl		0.44		
6	3-Pyridinyl		1.29	2.53	11.1
7	4-OHPh		0.33		
8	2,4 (OH) ₂ Ph		2.39	0.57	1.5
36	4-NO ₂ Ph		1.14		
C6	3-Pyridinyl	Ph	0	0.25	0.56
C8 ^d	2,4-(OH) ₂ Ph	Ph	1.16		
C28	Ph	4-NO ₂ Ph	0		
	Fc	Fc	5.2		
	Ph	Ph	0		
	Ferrocene		0.75	0.02	0.04

^a TEAC measures the ABTS^{•+} radical scavenging activity of test compound compared to Trolox.

^b Total amount of PBN-OH and PBN-CH₃ adducts produced during incubation (45 min, presence of air, 23 °C) of 100 μM test compound with PBN in DMSO (1%, v/v)-distilled water.

^c Rate of PBN adduct formation as determined from Fig. 5c.

^d TEAC of 2'-hydroxychalcone and 4'-hydroxychalcone are 0.66 and 0.26, respectively.

mation by selected compounds (1, 6, 8, 13, 27, 28) and ferrocene were explored by electron paramagnetic resonance (EPR) using two spin traps, α-phenyl-tert-butyl nitrone (PBN) and 5,5-dimethylpyrrolidine-N-oxide (DMPO).

The EPR spectra of a solution of DMPO and the test compound incubated at room temperature in the presence of oxygen exhibited a composite signal pattern indicative of the formation of hydroxyl and methyl adducts of DMPO (Fig. 5a). The formation of the DMPO-CH₃[•] adduct can be traced to the reaction of the solvent DMSO with the hydroxyl free radical (Tomasi and Iannone, 1993). Thus, the integral amount of both radicals was related to the amount of hydroxyl radical initially formed by the ferrocenyl chalcone. Fig. 5a was obtained using 1, but it is typical for the other test compounds. Incubation beyond 5 min caused a decrease in signal intensity due to the unstable nature of the DMPO adducts. A similar pattern was observed from the EPR spectra obtained from PBN and 1 (45 min incubation in air). A composite signal pattern characteristic of hydroxyl and methyl adducts of PBN was observed (Fig. 5b).

Fig. 5c shows the change in signal intensity of PBN adducts on incubation (45 min) with the test compound. In the case of compounds 6 and 13, the initial increase gradually reached a

plateau presumably because the adducts were unstable and participated in secondary reactions at high concentrations. The total amount of PBN adducts produced during the incubation period and the rates of their formation are given in Table 5. Unsubstituted ferrocene produced negligible levels of free radicals but incorporating the metallocene into the chalcone template enhanced radical formation. Compounds 6 and 13 produced the largest amounts of PBN adducts upon incubation. By contrast, the phenyl analogue of 6 (C6) produced an insignificant amount of radical adducts. There was a good correlation between the amount of free radicals formed and the rates at which they are generated.

In Fig. 6, the test compounds were ranked according to their abilities to produce PMN adducts, TEAC values and antiplasmodial activities. The longest bar indicated a compound that was highly ranked for each property (highest TEAC value, most active as antiplasmodial agent or produces the largest amount of free radical adducts). Compounds with high TEAC values were expected to be competent free radical generators since both processes involved an initial step of electron donation. This was generally true for the compounds tested, with the exception of 8 and 13. In the case of 8, it may be that the hydroxyl groups contributed significantly to the scavenging of

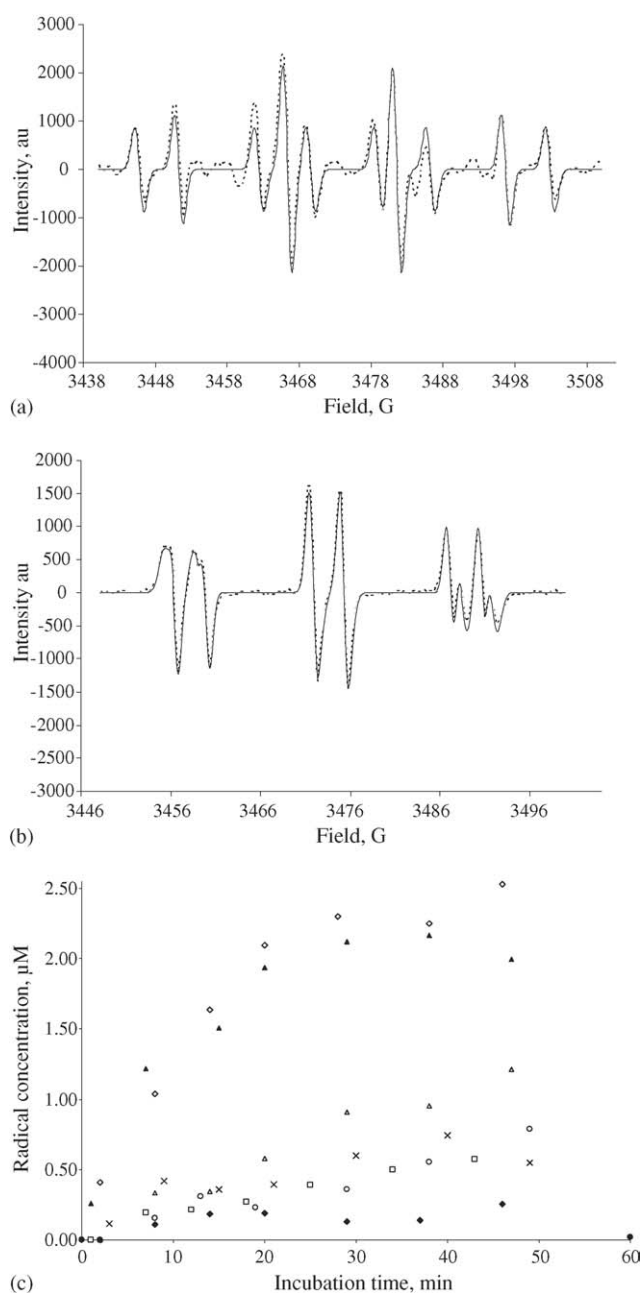


Fig. 5 – (a) EPR spectra of solutions containing DMPO (100 mM) and compound 1 (100 μM) in 1% (v/v) DMSO–water, incubated in the presence of the air for 5 min. Simulated spectra (bold line) were obtained by using parameters for hydroxyl adduct ($a_N = 14.9$, $a_H = 14.9$ G) and methyl adduct, $a_N = 16.6$, $a_H = 23.8$ G. Relative content of the hydroxyl adduct was 58, 57, 54, 46, 65 and 58% for compounds 1, 6, 8, 13, 27 and 28, respectively. The remaining was attributed to the methyl adduct. **(b)** EPR spectra of solutions containing PBN (100 mM) and compound 1 (100 μM) in 1% (v/v) DMSO–water, incubated in the presence of air for 45 min. Simulated spectra (bold line) were obtained by using: $a_N = 16.4$, $a_H = 3.3$ G (hydroxyl adduct 33, 33, 32, 29, 30, 29 and 33% for compounds C6, 1, 6, 8, 13, 27 and 28, respectively) and $a_N = 15.3$, $a_H = 3.5$ G (methyl adduct 67, 67, 68, 71, 70, 71, and 67% for compounds C6, 1, 6, 8, 13, 27

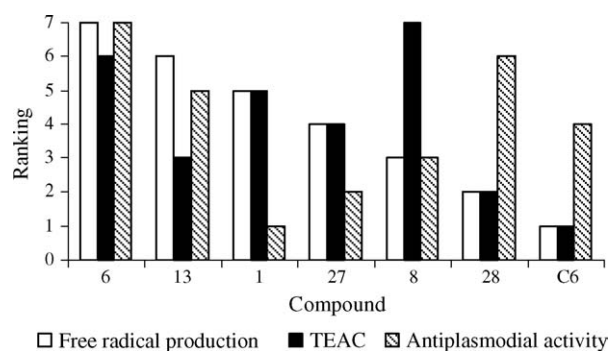


Fig. 6 – Ranking of compounds 1, 6, 8, 13, 27, 28 and C6 based on the total amount of radicals formed on incubation (45 min) with PBN, TEAC and antiplasmodial activity. For each category, the most potent/active compound is ranked (7) and the least potent/active compound is ranked (1).

ABTS^{•+} but played a lesser role in interacting with the spin trap to produce free radicals. No good reason can be proposed for the results obtained for 13.

The correlation between radical production and antiplasmodial activity was also examined. Compound 6 combined good antiplasmodial activity with a high level of radical production. Its phenyl analog C6 showed the opposite trend. This observation underscored an important role for ferrocene in free radical generation. Compounds 8 and 13 showed a satisfactory correlation between free radical production and antiplasmodial activity, but not compounds 1 and 28. Compound 28 belonged to series A and the resistance of ferrocene to oxidation (high E'_0) might account for the low levels of free radical generation. The antiplasmodial activity of 28 may arise from other factors that are not related to free radical formation. Another series A compound (27) also showed a mismatch between free radical generation and antiplasmodial activity. Compound 1 belonged to series B and its ferrocene ring had a lower E'_0 value. Thus, it was associated with a fairly high level of free radical formation, but for some reason, this did not translate to good antiplasmodial activity.

4. Discussion

The ferrocenyl chalcones investigated in this study demonstrated a wide range of antiplasmodial activity against a chloroquine resistant isolate of *P. falciparum*. The most active compounds were 6 and 28 which had IC_{50} values in the low micromolar range (4–5 μM). Compound 28 showed selective activity for plasmodia compared to mammalian cell lines MDCK (SI=14) and KB3-1 (SI=37). The selectivity indices for 6 were slightly lower, ranging from 5 to 9. In general, the mod-

and 28, respectively). **(c)** Free radical formation (hydroxyl and methyl adducts) obtained on incubation (presence of air) of the following compounds with PBN: 1 (Δ), 6 (◇), 8 (□), 13 (▲), 27 (○), 28 (×), C6 (◆), ferrocene (●).

est activity of the ferrocenyl chalcones was compensated to some extent by selective activity against plasmodia. Earlier acute and chronic toxicity tests attested to the relative safety of ferrocene and its derivatives in many mammalian species (Yeary, 1969; Leung et al., 1987; Nikula et al., 1993).

An important finding to emerge from the present investigation was the influence exerted by the location of ferrocene in the chalcone template on physicochemical properties and to some degree, the antiplasmodial activities of the ferrocenyl chalcones. Series A compounds in which ferrocene was ring A (adjacent to carbonyl moiety) were generally more active than their series B counterparts (ferrocene is ring B and adjacent to the α,β -unsaturated bond). Thus, for 15 pairs of compounds in which rings A and B were switched, the series A compound demonstrated better activity in nine pairs. PCA and PLS showed that the properties that were important for antiplasmodial activity also served to distinguish series A from series B compounds. The series A compounds were characterized by ferrocene rings in which Fe^{2+} was more resistant to electron loss (oxidation) and the presence of polarized carbonyl bonds. Chibale et al. (2000) noted that the antiplasmodial activity of urea and amine analogs of ferrochloroquine against the chloroquine sensitive *P. falciparum* D10 correlated well with the redox potentials of the ferrocene ring. Compounds with larger half-wave potentials (and thus ferrocene rings that were more resistant to oxidation) had better antiplasmodial activity, which was also observed in the present study. While the significance of these observations remains to be elucidated, the role of ferrocene was unlikely to be restricted to that of a hydrophobic spacer group or a substitute for phenyl. If ferrocene functioned only in this capacity, then its position as ring A or B should not influence antiplasmodial activity.

The QSAR findings prompted investigations into the oxidant role of ferrocene in selected ferrocenyl chalcones. Electron transfer from Fe^{2+} in ferrocenyl chalcones to a stable free radical $\text{ABTS}^{\bullet+}$ and to other reactive oxygen species which were detected as hydroxyl radicals of two spin traps, indicated that ferrocene participated in redox processes that involved the quenching and generation of free radicals. The fact that these processes were observed at significantly reduced rates in some non-ferrocenyl chalcones underscored an important role for the metallocene. At the same time, the observation that free radical generation was increased when ferrocene was incorporated into a chalcone suggests that the latter had a role in enhancing the oxidant properties of the metallocene.

Since Fe^{2+} was more readily oxidized when ferrocene is ring B, free radical generation should be greater among the series B compounds. Indeed, two (1, 6) of the three compounds that generated the most free radicals belonged to series B, but only 6 combined a high level of radical generation with good antiplasmodial activity. Although electrochemical measurements pointed to a less readily reduced ferrocene in series A, selected compounds (13, 27 and 28) in series A did generate free radicals in EPR experiments, albeit at a slower rate and in smaller amounts. While emphasis had been paid to the oxidant role of ferrocenyl chalcones, the physicochemical properties of series A and series B differed in other respects. Series A compounds had generally lower lipophilicities, more polarized carbonyl bonds and were more planar than series B compounds. The interaction of these properties, and not ox-

idant properties alone, may be important in considering the overall antiplasmodial profile of these compounds.

5. Conclusion

The purpose of the present study was to investigate the role of ferrocene in the antiplasmodial activity of ferrocenyl chalcones. Ferrocene could either play a structural role as a hydrophobic spacer or contribute in a more direct way via electron transfer involving Fe^{2+} . Based on the present results, a purely structural role was discounted as the position of ferrocene in the chalcone template influenced both the physicochemical properties and to some degree, the antiplasmodial activity of the compounds. Ferrocenyl chalcones demonstrated radical quenching properties and hydroxyl adduct formation in EPR experiments. Thus, the involvement of ferrocene in redox cycling seemed plausible and this process may contribute to the antiplasmodial activity of ferrocenyl chalcones. The location of the ferrocene ring influenced its susceptibility to oxidation as well as other physicochemical properties (lipophilicity, polarity and planarity). The interaction of these properties may determine the final antiplasmodial profile of the ferrocenyl chalcone.

Acknowledgement

Wu Xiang gratefully acknowledges research scholarship support from the National University of Singapore. This work was supported by Grants RP140000032112 and 000058112 (MLG); R143000213112 (ERTT) from National University of Singapore and the Thailand Research Fund (P.W.).

Appendix A. Supplementary data

Supplementary information: Analytical data (Tables 1 and 2), crystallographic data of compounds 1, 12 and 28 (Table 3) and physicochemical parameters (Table 4) of synthesized compounds.

Supplementary data associated with this article can be found, in the online version, at doi:10.1016/j.ejps.2005.09.007.

REFERENCES

- Alley, M.C., Scudiero, D.A., Monks, A., Hursey, M.L., Czerwinski, M.J., Fine, D.L., Abbott, B.J., Mayo, J.G., Shoemaker, R.H., Boyd, M.R., 1988. Feasibility of drug screening with panels of human tumour cell lines using a microculture tetrazolium assay. *Cancer Res.* 48, 589–601.
- Aston, J.Y., Fry, A.J., 2004. Substituent effects on the reduction potentials of benzalacetophenones (chalcones). Improved substituent constants for such correlations. *Electrochem. Acta* 49, 455–459.
- Atteke, C., Ndong, J.M.M., Aubouy, A., Maciejewski, L., Brocard, J., Lebib, J., Deloron, P., 2003. In vitro susceptibility to a new antimalarial organometallic analogue, ferroquine, of *Plasmodium falciparum* isolates from the Haut-Ogooue region of Gabon. *J. Antimicrob. Chemother.* 51, 1021–1024.

- Beagley, P., Blackie, M.A.L., Chibale, K., Clarkson, C., Meijboom, R., Moss, J.R., Smith, P.J., Su, H., 2003. Synthesis and antiparasitic activity in vitro of new ferrocene–chloroquine analogues. *Dalton Trans.*, 3046–3051.
- Beurskens, P.T., Admiraal, G., Beurskens, G., Bosman, W.P., García-Granda, S., Smits, J.M.M., Smykalla, C., 1992. The DIRDIF Program System, Technical report of the Crystallography Laboratory. University of Nijmegen.
- Blessing, R., 1995. An empirical correction for absorption anisotropy. *Acta Crystallogr., Sect. A* 51, 33–38.
- Biot, C., Delhaes, L., Maciejewski, L., Mortuaire, M., Camus, D., Dive, D., Brocard, J.S., 2000. Synthetic ferrocenic mefloquine and quinine analogues as potential antimalarial agents. *Eur. J. Med. Chem.* 35, 707–714.
- Chibale, K., Moss, J.R., Blackie, M., van Schalkwyk, D., Smith, P.J., 2000. New amine and urea analogs of ferrochloroquine: synthesis, antimalarial activity in vitro and electrochemical studies. *Tetrahedron Lett.* 41, 6231–6235.
- Chim, P., Lim, P., Sem, R., Nhem, S., Maciejewski, L., Fandeur, T., 2004. The in-vitro antimalarial activity of ferrochloroquine, measured against Cambodian isolates of *Plasmodium falciparum*. *Ann. Trop. Med. Parasitol.* 98, 419–424.
- Delhaes, L., Abessolo, H., Biot, C., Berry, L., Delcourt, P., Maciejewski, L., Brocard, J., Camus, D., Dive, D., 2001. In vitro and in vivo antimalarial activity of ferrocene–chloroquine, a ferrocenyl analogue of chloroquine against chloroquine-resistant malaria parasites. *Parasitol. Res.* 87, 239–244.
- Delhaes, L., Biot, C., Berry, L., Maciejewski, L., Camus, D., Brocard, J.S., Dive, D., 2000. Novel ferrocenic artemisinin derivatives: synthesis, in vitro antimalarial activity and affinity of binding with ferroprotoporphyrin IX. *Bioorg. Med. Chem.* 8, 2739–2745.
- Dimmock, J.R., Kandepu, N.M., Hetherington, M., Wilson Quail, J., Pugazhenti, U., Sudom, A.M., Chamankhah, M., Rose, P., Pass, E., Allen, T.M., Halleran, S., De Clercq, E., Balzarini, J., 1998. Cytotoxic activities of Mannich bases of chalcones and related compounds. *J. Med. Chem.* 41, 1014–1026.
- Dimmock, J.R., Zello, G.A., Oloo, E.O., Wilson Quail, J., Kraatz, H., Perjesi, P., Aradi, F., Takacs-Novak, K., Allen, T.M., Santos, C.L., Balzarini, J., De Clercq, E., Stables, J.P., 2001. Correlations between cytotoxicity and topography of some 2-arylidenebenzocycloalkanones determined by X-ray crystallography. *J. Med. Chem.* 45, 3103–3111.
- Domarle, O., Blampain, G., Agnani, H., Nzadiyabi, T., Lebibi, J., Brocard, J., Maciejewski, L., Biot, C., Georges, A.J., Millet, P., 1998. In vitro antimalarial activity of a new organometallic analog, ferrocene–chloroquine. *Antimicrob. Agents Chemother.* 42, 540–544.
- Hocek, M., Stepnicka, P., Ludvik, J., Cisarova, I., Votruba, I., Reha, D., Hobza, P., 2004. Ferrocene-modified purines as potential electrochemical markers: synthesis, crystal structures, electrochemistry and cytostatic activity of (ferrocenylethynyl-) and (ferrocenylethyl) purines. *Chem. Eur. J.* 10, 2058–2066.
- Itoh, T., Shirakami, S., Ishida, N., Yamashita, Y., Yoshida, T., Kim, H.S., Wataya, Y., 2000. Synthesis of novel ferrocenyl sugars and their antimalarial activities. *Bioorg. Med. Chem. Lett.* 10, 1657–1659.
- Leung, H.W., Hallesy, D.W., Shott, L.D., Murray, F.J., Paustenbach, D.J., 1987. Toxicological evaluation of substituted dicyclopentadienyliron (ferrocene) compounds. *Toxicol. Lett.* 38, 103–108.
- Li, R., Kenyon, G.L., Cohen, F.E., Chen, X., Gong, B., Dominguez, J.N., Davidson, E., Kurban, G., Miller, R.E., Nuzum, E.O., Rosenthal, P.J., McKerrow, J.H., 1995. In vitro antimalarial activity of chalcones and their derivatives. *J. Med. Chem.* 38, 5031–5037.
- Liu, M., Wilairat, P., Go, M.L., 2001. Antimalarial alkoxyated and hydroxylated chalcones: structure activity relationship analysis. *J. Med. Chem.* 44, 4443–4452.
- Livingstone, D., 1995. *Data Analysis for Chemists*. Oxford University Press, Oxford.
- Lopez, S.N., Castelli, M.V., Zacchino, S.A., Dominguez, J.N., Lobo, G., Charris-Charris, J., Cortes, J.C.G., Ribas, J.C., Devia, C., Rodriguez, A.M., Enriz, R.D., 2001. In vitro antifungal evaluation and structure-activity relationships of a new series of chalcone derivatives and synthetic analogues with inhibitory properties against polymers of the fungal cell wall. *Bioorg. Med. Chem.* 9, 1999–2013.
- Nielsen, S.F., Kharazmi, A., Christensen, S.B., 1998. Modification of the α,β -double bond in chalcones only marginally affect the antiprotozoal activities. *Bioorg. Med. Chem.* 6, 937–945.
- Nikula, K.J., Sun, J.D., Barr, E.B., Bechtold, W.E., Haley, P.J., Benson, J.M., Eidson, A.F., Burt, D.G., Dahl, A.R., Henderson, R.F., 1993. Thirteen-week repeated inhalation exposure of F344/N rats and B6C3F1 mice to ferrocene. *Fund. Appl. Toxicol.* 21, 127–139.
- Ong, C.W., Jeng, J.Y., Juang, S.S., Chen, C.F., 1992. A ferrocene-intercalator conjugate with a potent cytotoxicity. *Bioorg. Med. Chem. Lett.* 2, 929–932.
- Osella, D., Ferrali, M., Zanello, P., Laschi, F., Fontani, M., Nervi, C., Caviglioglio, G., 2000. On the mechanism of the antitumour activity of ferrocenium derivatives. *Inorg. Chim. Acta* 306, 42–48.
- Rastelli, G., Antolini, L., Benvenuti, S., Costantino, L., 2000. Structural bases for the inhibition of aldose reductase by phenolic compounds. *Bioorg. Med. Chem.* 8, 1151–1158.
- Re, R., Pellergrini, N., Proteggente, A., Pannala, A., Yang, M., Rice-Evans, C., 1999. Antioxidant activity applying an improved ABTS radical cation decolorization assay. *Free Radical Biol. Med.* 26, 1231–1237.
- Sheldrick, G.M., 1997. *SHELXL97 Program for the Refinement of Crystal Structures*. University of Göttingen.
- Silverstein, R.M., Webster, F.X., 1997. *Spectrometric Identification of Organic Compounds*. John Wiley & Sons, New York.
- Swarts, J.C., Swarts, D.M., Maree, D.M., Neuse, E.W., La Madeleine, C., Van Lier, J., 2001. Polyaspartamides as water-soluble drug carriers. Part 1. Antineoplastic activity of ferrocene-containing polyaspartamide conjugates. *Anticancer Res.* 21, 2033–2038.
- Tomasi, A., Iannone, A., 1993. ESR Spin trapping artifacts in biological systems. In: Berliner, L.J., Jacques, R. (Eds.), *Biological Magnetic Resonance, EMR of Paramagnetic Molecules*, Vol13. Plenum Press, New York, pp. 353–384.
- Top, S., Vessieres, A., Cabestaing, C., Laïos, I., Leclercq, G., Provot, C., Jaouen, G.J., 2001. *Organomet. Chem.* 637–639, 500–506.
- Top, S., Vessieres, A., Leclercq, G., Quivy, J., Tang, J., Vaissermann, J., Huche, M., Jaouen, G., 2003. Synthesis, biochemical properties and molecular modeling studies of organometallic specific estrogen receptor modulators (SERMs), the ferrocifens and hydroferrocifens. Evidence for an antiproliferative effect of hydroxyferrocifens on both hormone-dependent and hormone-independent breast cancer cell lines. *Chem. Eur. J.* 9, 5223–5236.
- Wu, X., Wilairat, P., Go, M.L., 2002. Antimalarial activity of ferrocenyl chalcones. *Bioorg. Med. Chem. Lett.* 12, 2299–2302.
- Yeary, R.A., 1969. Chronic toxicity of cyclopentadienyliron (ferrocene) in dogs. *Toxicol. Appl. Pharmacol.* 15, 666–676.